

THE SUCTION PERFORMANCE OF CENTRIFUGAL PUMPS POSSIBILITIES AND LIMITS OF IMPROVEMENTS

by

Peter Hergt

Senior Research Engineer

Alexander Nicklas

Head of Hydraulic Development Department

Gerhard Mollenkopf

Head of Experimental Research of New Technologies

and

S. Brodersen

Head of Hydraulic Research and Development

KSB Aktiengesellschaft

Frankenthal, Germany



Peter Hergt is Senior Research Engineer and Vice Director of the "New Technologies" division. He received his Engineering Diploma in 1960 from the Technical University of Karlsruhe, Germany. After joining KSB Aktiengesellschaft, Frankenthal, Germany, in 1960 he dealt with hydraulic basic research. Between 1975 and 1988, Mr. Hergt was head of the Central Hydraulic Research and Development Department

and was responsible for the hydraulic design of all pumps within the KSB program.



Gerhard Mollenkopf is head of Experimental Research of the New Technologies division of KSB Aktiengesellschaft, Frankenthal, Germany. His responsibilities include customer support in examining pump problems in situ. Dr. Mollenkopf joined KSB's research center in 1971 and was involved in the design and construction of the experimental research center. Dr. Mollenkopf received his Ph.D. at the University of Munich with a dissertation on

cavitation problems in water turbines.



Alexander Nicklas heads the Hydraulic Development Department of the New Technologies division of KSB Aktiengesellschaft, Frankenthal, Germany. His responsibilities are the development and improvement of hydraulic products, with major emphasis on heavy-duty pumps for power engineering applications. Mr. Nicklas joined KSB's fluid dynamics research center in 1974 with responsibility for the development of improved vane profiles to reduce the risk of cavitation damage to boiler feed pumps.

He has many years' experience in the hydraulic improvement of multistage pumps and in fundamental research in the field of

cavitation erosion. Mr. Nicklas received his Mechanical Engineering degree at Darmstadt Technical University, Germany, where hydraulic machinery and plant engineering were the major fields of his studies.

ABSTRACT

Following a brief description of the general suction performance of pumps and starting from an impeller designed for standard requirements, it will be discussed by which modifications and up to which limit the suction performance can be improved.

In this context, it will be shown that the well-known measures – e.g., enlargement of the impeller inlet diameter, reduction of the vane number or installation of an inducer – may result in some restrictions concerning the possible operational range and may pose a risk of cavitation erosion. These undesirable consequences can, however, be avoided or at least moderated by modifications upstream of the impeller.

The suction performance can also be improved by using double suction instead of single suction pumps. It is explained why the resulting improvement may not be as substantial as could be assumed at a first glance.

Pumps with inlet velocities exceeding 25 to 30 m/s that are expected to run for 10,000 hr and more without cavitation damage cannot operate at NPSH values corresponding to a 3.0 percent head drop, even if a highly cavitation-resistant material is used. It is demonstrated that the design parameters of their impellers differ from those used for 'normal' impellers.

If NPSHA is not sufficient, a booster pump has to be provided, or the rotational speed has to be reduced. As the latter is an expensive alternative, the question arises what the minimum booster pump head is. Some information regarding this issue is given.

It will also be demonstrated that there is an upper limit of the rotational speed of the main pump beyond which an economical solution is impossible.

INTRODUCTION

A major factor in plant engineering, be it for process circuits, water supply, or power generation applications, is the NPSH required by the pump used, which greatly influences the system's design and cost. It goes without saying that large, low-speed machines, possibly connected in parallel or in multistage design, with their low NPSH requirement are a safe solution in terms of

plant cost and operating reliability, but such machines come expensive and the system will not operate economically. With a view to optimizing cost on the one hand and ensuring operating reliability and availability on the other, the plant designer needs a thorough understanding of the cavitation-dependent operation limits.

An outline is provided of the characteristic properties of centrifugal pumps in this respect and their application limits as defined by the latest findings in the field of fluid dynamics. On the one hand, it describes the basic phenomena that occur in an impeller, if the system NPSH falls below a specific pump- and load-dependent value. On the other hand, it is to demonstrate which $NPSH_{req}$ value cannot be underrun in a specific case and with a specific pump.

A brief description of the interrelations between the impeller's geometry and its cavitation and operating characteristics is to help the operator retrace the steps taken and gain a better understanding of the factors limiting the operating range.

GENERAL REMARKS ON THE HYDRODYNAMIC CAVITATION CHARACTERISTICS OF CENTRIFUGAL PUMPS

Discharge Head

In Figure 1, the NPSH curves for incipient cavitation ('i'), 0 percent, 3.0 percent and total head breakdown (bd) are shown. The latter is characterized by a steep head drop at constant flow rate and is normally not measured. Although the numerical values apply to a specific pump and cannot be easily generalized, a few universal conclusions can be drawn:

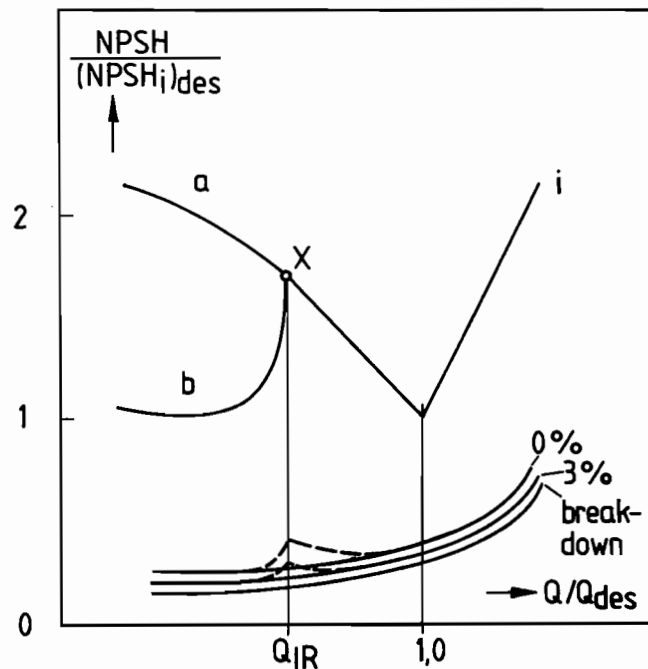


Figure 1. Typical NPSH Curves of Pumps.

- $NPSH_i$ has a minimum at the point for which the impeller inlet has been designed (Q_{des}). This need not necessarily coincide with the pump's best efficiency point (Q_{BEP}).
- The curves defined on the basis of the head drop criterion lie far below the $NPSH_i$ curve and have a different shape.

Evaluation of numerous tests showed that the following approximate ranges can be given for $Q/Q_{des} = 1.0$.

$NPSH_i/NPSH_3$	≈ 2.0 for special vane profiles
	$= 4$ to 6 for standard designs
	≈ 8 to 10 for impellers with a low number of vanes ($z = 3$)
$NPSH_0/NPSH_3$	$= 1.1$ to 1.3
$NPSH_{bd}/NPSH_3$	$= 0.8$ to 0.9 for standard impellers
	≈ 1.0 for impellers with high S_q (NSS)

- $NPSH_i$ increases sharply and almost linearly with Q in the off-design operating ranges.

After point X, which marks the onset of recirculation at the impeller inlet (Q_{IR}), $NPSH_i$ increases further (curve a), if elements disturbing the development of recirculation are installed upstream of the impeller. Such elements are, for example, axial ribs inserted to stabilize the characteristic curve or a bend immediately upstream of the pump.

If a cylindrical pipe without any inserts is fitted upstream of the impeller, $NPSH_i$ drops sharply at Q_{IR} to a level that roughly corresponds to that of the design point. The reason for this phenomenon is that the cavitation zone moves from the shroud zone into the hub area, where the velocity level is lower.

The curves shown in Figure 1 are typical for overhung impellers and basically also for impellers where the shaft is led through the impeller eye (multistage or double-suction pumps), as long as $n_q < 60$ ($N_s < 3100$) and $D_h/D_1 < 0.6$. Impellers with higher specific speeds $n_q > 70$, and $D_h/D_1 > 0.6$ sometimes exhibit peaks in the $NPSH_0$ and $NPSH_3$ curves near Q_{IR} (broken lines in Figure 1).

In this flow range, the head already decreases if the cavitation zone is relatively short compared with other flow ranges. As described by Kosyna [1], this is the result of a cavitation-induced change in the flow through the impeller combined with poorer energy transformation. Accurate measurements typically reveal these pumps' characteristic curves to have discontinuities at Q_{IR} even under non-cavitating conditions [2, 3].

The basic correlation between the development of the cavitation zone and decreasing NSPH (σ_u) is illustrated in Figure 2. Starting at σ_{u1} , the cavitation zone grows with decreasing σ_u , first slowly and then ever more rapidly, more or less following a hyperbolic curve. The value of the pitch-related bubble length $I_B/t = 1.0$ roughly corresponds to a 3.0 percent head drop. In accordance with Figure 1, cavity growth at low flow ($Q/Q_{des} = 0.75$) starts at higher σ_u and reaches $I_B/t = 1$ (corresponding to $\Delta H/H = 3$ percent) at lower σ_u compared with the design point.

In Figure 3, another correlation is shown. The head related to the head for noncavitating operation (H_{cf}) is plotted against the relative cavitation zone length. At the design point Q_{des} , H remains completely unaffected up to approximately $I_B/t = 0.35$ and then decreases continuously. At low flow, H remains unaffected up to $I_B/t = 0.6$, and then drops relatively sharply. This could give the impression of greater safety at low flow, which is not true, however, as will be shown later.

All previous data referred to impellers with vanes symmetrically tapered at the inlet (b in Figure 4). If the vanes are tapered asymmetrically, either on the suction (SS) or on the pressure side (PS), this will have a significant effect on σ_{u1} , and a weaker, yet perceptible effect on σ_{u3} , as shown in Figure 5.

Sharpening on the vane's pressure side does improve the σ_{u3} value at large flowrates, but σ_{u1} also increases substantially. This may put the pump at risk, if erosion phenomena have to be taken into account. Sharpening on the suction side reduces the σ_{u1} values,

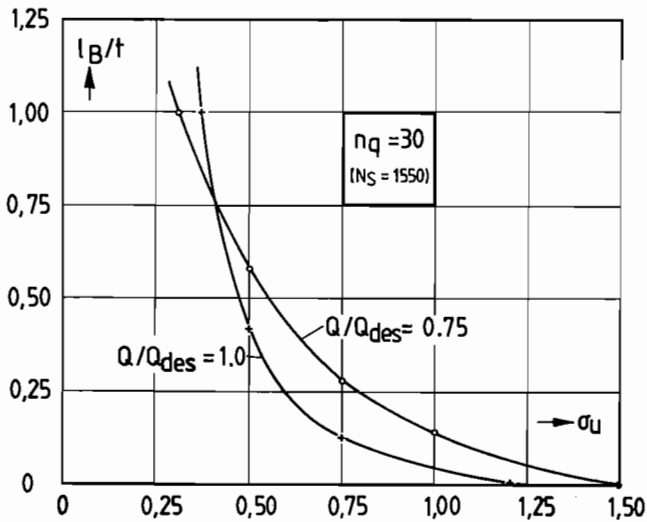


Figure 2. Cavitation Zone Length l_B (Related to Pitch t) vs Cavitation Coefficient σ_u .

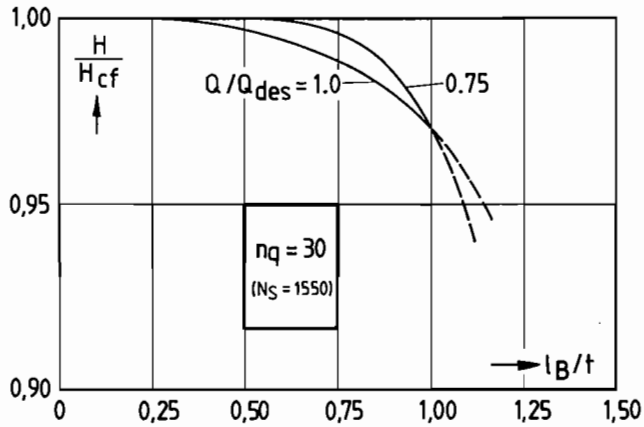


Figure 3. Pump Head Related to Cavitation-Free Operation (c_f) Plotted Against Dimensionless Cavitation Zone Length l_B/t at Design Point and Low Flow Operation.

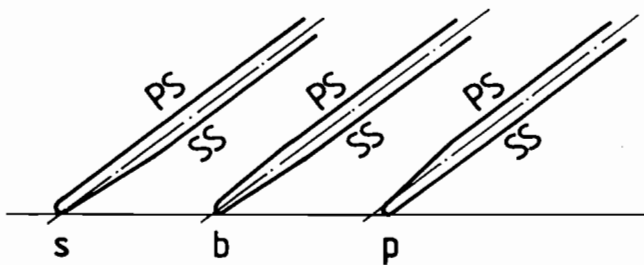


Figure 4. Different Vane Leading Edge Contours, PS = Pressure Side, SS = Suction Side.

in particular at low flow and improves, though just slightly, σ_{u3} , for very low flowrates.

However, cutting back the vane inlet edge by some millimeters and then tapering the vane from the suction or the pressure side is a measure that can be taken onsite, if the desired changes in the cavitation performance are within the range shown in Figure 5.

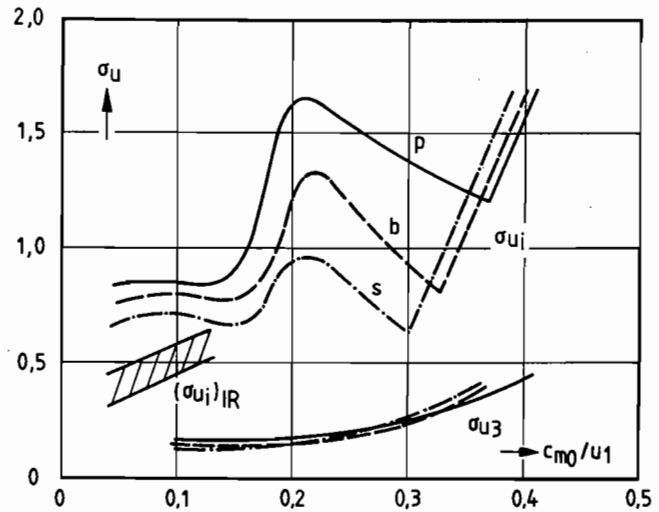


Figure 5. Cavitation Coefficient σ_u for Different Vane Leading Edge Contours (Figure 4) Plotted Against Flowrate Number c_{m0}/u_1 .

Efficiency

The change in efficiency with decreasing NPSH depends on the type of blading (solidity) and the operating point, although exact correlation have not yet been established.

Often the head drop is accompanied by a slight rise in the power input (0 percent $\leq \Delta P \leq 1.5$ percent), which results in a somewhat higher efficiency reduction than head drop.

CAVITATION EROSION

Whether appreciable damage occurs or not depends on the hydrodynamic cavitation intensity (HCI) on the one hand and the material's cavitation erosion resistance (CR) on the other.

As far as materials are concerned, the authors have at least a general idea of the quantitative relationships between the erosion velocities of different materials. In Table 1, these ratios are listed for a few selected materials.

Table 1.

Material	Relative Erosion
Grey cast iron (GCI)	9.2
Bronze G-CuSn10	3.3
Bronze CuAl10Ni	1.3
A 743 CF-8M, 316 ss	1.0
A 351 CD 4M CU	0.7
TiAlV6	0.6
Stellite 6	0.05

This means that in some cases a change of the impeller material can eliminate or at least moderate erosion problems. An impeller made of G-CuSn10 will have a lifetime approximately three times longer than that of a GCI impeller.

What is harder to assess is the effect of hydrodynamic cavitation intensity, which has not yet been exactly defined with all its influencing parameters. Although the authors do know that the following parameters affect cavitation intensity, there is not enough data of their influence for given fluid properties:

- the flow velocity at the location where cavitation occurs
- the cavitation zone volume or the cavitation zone length
- the pressure gradient at the end of the cavitation zone
- the model size

Since local flow velocity and the pressure gradient at the end of the cavitation zone for a given impeller geometry are a function of the inlet flow angle, these two variables include the influence of the relative load point.

As local flow velocity is not known in most cases, it is replaced by the average inflow velocity w_1 , which is an acceptable approximation provided a uniform design concept is used. For comparative studies the rate of erosion E_R is taken to be - depending on this velocity and the cavitation zone or bubble length I_B -

$$E_R = C(I_B)^a \cdot (w_1)^b \tag{1}$$

for given material and fluid properties. The constant C includes the local velocity peak and the pressure gradient influence, i.e., it is a function of the operating point. According to an EPRI report [4] it is possible to set $a \approx 2.8$ and $b \approx 6$, which gives

$$E_R = C(I_B)^{2.8} \cdot (w_1)^6 \tag{2}$$

Systematic pump test series have shown that the erosion rate with $I_B = \frac{\pi D_1}{z}$ is negligible up to $w_1 = w_{1,crit} \approx 12\text{m/s}$ or cast iron and up to $w_{1,crit} \approx 22\text{m/s}$ for stainless steel 316 ss. This finding and the above equation yield Figure 6, which applies to $Q \approx Q_{des}$. For higher w_1 , additional corrections resulting from practical experience were made. Like the constant C, the critical velocities $w_{1,crit}$ are a function of the operating point and must be assumed for $Q < Q_{des}$ to be lower.

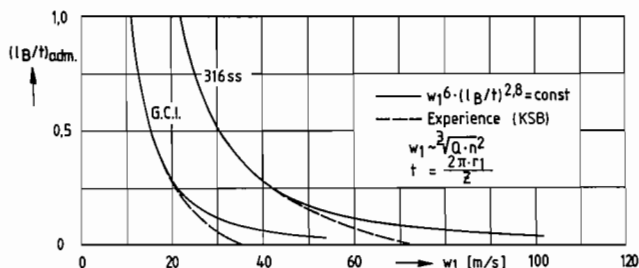


Figure 6. Admissible Dimensionless Cavitation Zone Length I_B/t for Different Materials as a Function of the Relative Inlet Velocity w_1 , $Q = Q_{des}$.

What is very difficult is the prediction of potential cavitation damage at $Q < Q_{IR}$, i. e., for flowrates with recirculation at the impeller inlet.

Although the vane cavitation zone moves into the impeller hub area (i.e., into an area of lower velocities w_1) as described for example by Schiavello and Sen [5], erosion phenomena may also occur in this region as a consequence of considerable inlet flow deviations on the vane suction side and marked pressure gradients. Hence, if an impeller shows cavitation erosion in the corner between the hub and the vane suction side, it will have run at $Q \leq 0.6 \cdot Q_{des}$.

The cavitation zones inside the vortex region depend on the recirculation intensity and are difficult to predict owing to the com-

plexity of flow details involved. They may cause erosion damage both on the vanes (in particular the vane pressure side) and on the elements upstream of the impeller. Measurements on a number of pumps revealed that the NPSH value for incipient cavitation in the recirculation regime is lower for undisturbed flow, for example, through a long cylindrical suction pipe, than for vane cavitation. Referred to curve b in Figure 5, the following would apply:

$$\text{at } c_{mo} / u_1 = 0.05 \quad (\sigma_{ui})_{IR} = 0.4$$

$$\text{at } c_{mo} / u_1 = 0.13 \quad (\sigma_{ui})_{IR} = 0.6$$

The cavitation zone length IB/t at the vanes would then already range at about 0.35.

PERFORMANCE OF STANDARD IMPELLERS

Most of the pumps produced today have to meet a variety of different requirements. While, for example, cavitation is of minor significance for primary circulating pumps in power stations, but a major factor for booster pump operation, common industrial or water supply pumps must cater for the most varied applications. As well as good (even though not exceptional) suction characteristics, they need to achieve high efficiency and a long service life. The suction behavior is just one parameter; the pump designer is expected to arrive at an optimum compromise between efficiency, operating behavior and suction characteristics.

The impeller eye diameter may be defined with the following equation derived from the affinity law $Q \sim n \cdot D_1^3$.

$$D_1 = \delta \sqrt[3]{\frac{Q/n}{1-v^2}} \text{ [m]} \quad v = D_H/D_1 \tag{3}$$

inserting the flowrate Q in m^3/s and the speed n in rpm. δ is then the inlet diameter in m of a geometrically similar pump with $Q = 1 \text{ m}^3/\text{s}$ and $n = 1 \text{ rpm}$.

Keeping the efficiency in mind, δ is chosen to be relatively small (also see *Enlarging the Inlet Diameter*), since small inlet diameters permit to use small sealing clearance diameters and thus, at a clearance width prescribed by the production process, result in lower internal leakage losses and higher efficiency.

From Equation (3) and from $\tan \beta_0 = c_{mo}/u_1$ it can easily be derived, that the inlet flow angle β_0 is defined by:

$$\tan \beta_0 = \frac{240}{\pi^2 \delta^3} \tag{4}$$

This angle, and consequently, the vane inlet angles become relatively large ($\beta_0 = 20^\circ - 22^\circ$). The small inlet diameter reduces friction losses in the vane passage due to the lower relative velocity.

The NPSH required calculated using the approach suggested by Pfleiderer [6]

$$\text{NPSH} = \lambda_c \cdot \frac{c_1^2}{2g} + \lambda_w \cdot \frac{w_1^2}{2g} \tag{5}$$

with $\lambda_c = 1.1 - 1.2$ and λ_w , according to Figure 7 then yields suction specific speed values

$$s_q = n \cdot \frac{\sqrt{Q}}{\text{NPSH}^{3/4}} \tag{6}$$

ranging at about 220 ($\text{NSS} \approx 11,000$), if δ is taken to be $\delta = 4.3 \text{ m}$ (Figure 8).

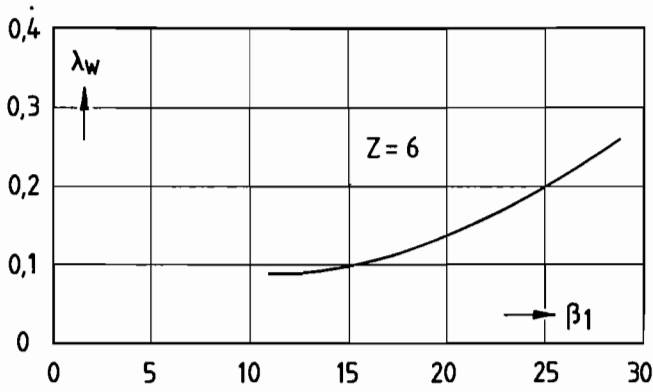


Figure 7. Coefficient λ_w vs Vane Inlet Angle β_1 .

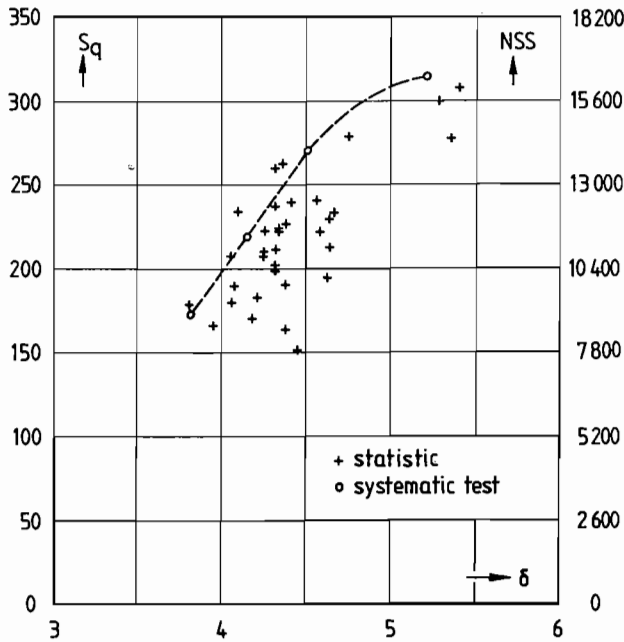


Figure 8. Suction Number S_q vs Specific Inlet Number δ .

Aimed at ensuring low-loss energy transfer, the number of vanes of standard impellers ranges between 5.0 and 8.0 in the low to medium specific speed range, i.e., it is higher than that of suction stage impellers (see *Reducing the Number of Vanes*).

NPSH plotted against the flowrate yields a curve similar to that illustrated in Figure 1. Under *Enlarging the Impeller Diameter*, it will be shown that higher suction specific speeds S_q require smaller vane angles and lower meridional velocities and, thus, larger suction diameters. This fact contradicts the interrelations described above for achieving high efficiency. Optimum efficiency and optimum suction characteristics, especially at below-design flows, are therefore mutually exclusive and cannot be combined in one pump.

Another characteristic feature of standard impellers is their good off-design efficiency compared with suction stage impellers. One reason for this is that with reduced inlet diameters, the inlet recirculation develops at lower Q/Q_{des} (also see section 6) and the energy imparted by the impeller to the recirculatory flow at the inlet

$$P_{IR} = k \cdot n^3 \cdot D_1^5 \sim \delta^5 \quad (7)$$

is considerably smaller than in suction stage impellers ($\delta = 4.7 - 5.2$ m).

METHODS OF IMPROVING THE SUCTION CHARACTERISTICS IN THE DESIGN FLOW RANGE

If the NPSH₃ value corresponding to the above-mentioned S_q value of 220 (NSS = 11,000) is not sufficient, performance can be improved in a number of ways, which can also be combined as described below.

Enlarging the Impeller Inlet Diameter

In Figure 8, a statistical evaluation of suction specific speeds S_q as a function of the inlet number δ along with the results of a systematic test series are presented. The results are plotted in Figure 9 of the systematic test series in dimensionless form vs the relative flowrate. Based on these curves with $\text{tg } \beta_0$ according to Equation (4) and

$$\text{tg } \beta_1 = \text{tg } \beta_0 \cdot \frac{\mu}{q} \quad (8)$$

with $\mu = 1.1$ representing a 10 percent incidence and $q \approx 0.9$ representing the ratio of net to total inlet area (vane blockage), Equation (5) yields a λ_w curve as shown in Figure 7 ($\lambda_c = 1.1$). Here the reference velocity is the relative velocity at the inlet diameter, which has a decisive influence on the suction characteristics and the cavitation erosion potential (location of highest relative velocity). This simplification does not quite give an adequate account of the changes in the velocity triangles resulting from the increase in diameter (Figure 10).

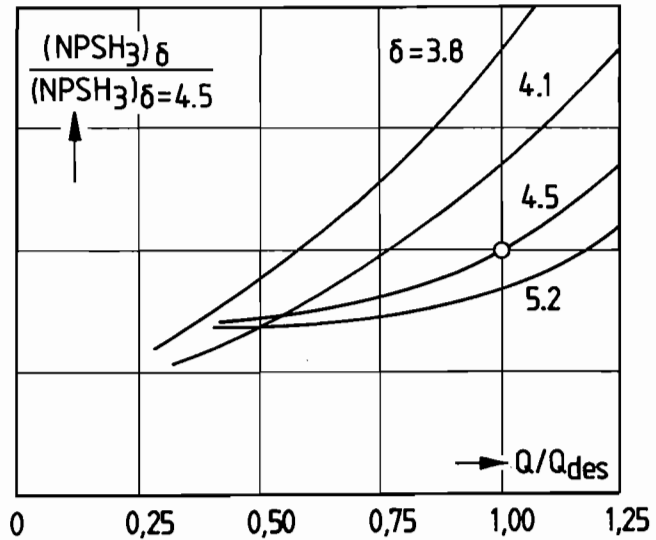


Figure 9. NPSH Plotted Against Flowrate for Different Specific Inlet Numbers δ (m) According to Equation (3).

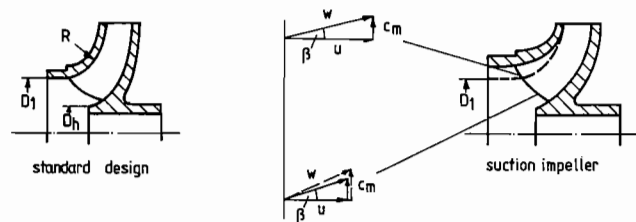


Figure 10. Standard and Suction Impeller, Corresponding Velocity Triangles.

A larger diameter D_1 results in a higher relative velocity in the added vane area (Figure 10), which however increases slightly less than linearly with the circumferential speed or D_1 , since the meridional velocity is reduced at the same time (assumption: $c_m = \text{const.}$ along the leading edge). The lower meridional velocity causes a reduction of relative velocity in the previous inlet area (corresponding to the standard impeller area), which in turn reduces the risk of cavitation erosion. This small improvement is indirectly included in the λ_w obtained from the measurements. For meridional section design, small curvatures are recommended, i.e., large radii and vanes extending far into the impeller eye. This will result in reduced local vane circulation and lower velocity peaks, which will have a positive effect on the complete NPSH_1 to NPSH_3 range and on cavitation erosion.

Considering the characteristics of the limit curve shown in Figure 8, it can be concluded that a further enlargement of D_1 will not yield any further perceptible reduction in NPSH. An impeller with a large diameter D_1 is, of course, more likely to be affected by cavitation erosion. In principle, these impellers are also prone to recirculation, since the inception point Q_{IR} may be located quite close to Q_{des} , as was shown by Fraser [7]. However, on the one hand the corresponding correlations have not yet been clearly defined, and on the other hand, methods are available that permit safe operation even below Q_{IR} (see *Improvements in the Low-Flow Range*).

Apart from the lower efficiency of suction impellers at reduced flowrates previously mentioned, the more or less unsteady power consumption caused by inlet recirculation can lead to vibrations depending on the overall design of the pump. In order to obtain first information about the risk of trouble, it is recommended to evaluate δ from Equation (3) with $Q = Q_{\text{des}}$. For $\delta < 4.5$, the risk is limited. For $\delta \geq 4.6$ the risk increases, if the pump is run below $0.7 \cdot Q_{\text{des}}$. This is true for low to medium specific speeds and for pumps above a certain size.

Reducing the Number of Vanes

A reduction in the number of vanes enlarges the free flow cross section area and, thus, improves NPSH_3 (Figure 11). Three or four vanes are, however, the minimum so as to avoid excessive loads on the vanes (see *Discharge Head*). In order to be able to maintain the original discharge head, the impeller is equipped with the full number of vanes from the middle of its passage to the outlet area, which means that the impeller has, for example, three long and three short vanes (called splitters). It must be kept in mind that a reduced number of vanes will increase the risk of low-frequency pressure fluctuations in the low flow range (see *Swift Control*).

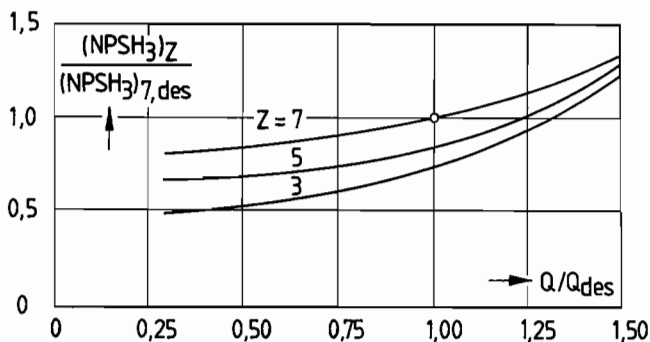


Figure 11. Influence of Vane Number z on NPSH.

Double-Suction Impellers

Should the suction impeller's NPSH_3 value still be insufficient for a very small NPSH_A , double-suction impellers (Figure 12) can

be used. The overall inlet area is approximately 20 percent larger than that of a single-suction impeller and NPSH_3 can be reduced by 30 percent on average. These values result from applying the following equations

$$A = \frac{\pi}{4} \cdot D_1^2 (1-v^2); D_1 = \delta \cdot \left(\frac{Q/n}{1-v^2} \right)^{1/3}; \delta = \text{const.} \quad (9)$$

and by variation of the hub ratio $v = D_h/D_1$ (Table 2).

The improvement resulting from the assumption that $\sigma_{\text{ud}} = \sigma_{\text{us}}$ can be attributed to the lower relative velocity level.

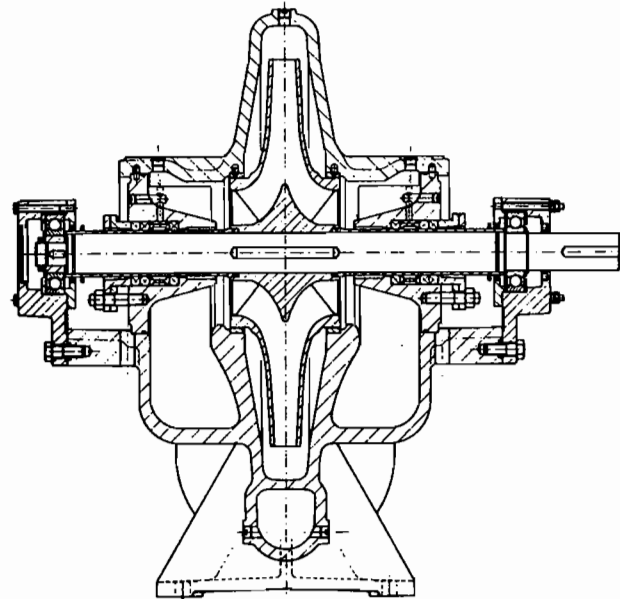


Figure 12. Typical Double-Suction Pump.

Initially, the above considerations (Table 2) did not take into account that NPSH_3 might increase due to the hub. In Figure 13, it is illustrated that the hub ratio D_h/D_1 has a significant effect on the NPSH_3 value. If this is allowed for, the values given in the last line are derived. In addition, it must be kept in mind that the improvement derived on the basis of these simple relationships will not quite be achieved in practice owing to

- losses in the inlet bend,
- distorted inlet flows to the impeller (90 degrees bending around the shaft).

Therefore, the values of double-suction impellers can be increased by approximately 5 percent.

Maximum S_q values referred to the total flowrate therefore only range at 350 ($\text{NSS} \approx 18,000$) ($v \leq 0.45$). In extreme cases, a double-suction pump with thick hub will not give better results than a single-stage pump without hub, at least as far as the NPSH_3 value is concerned. NPSH_1 values are improved due to the reduced relative velocity level.

When considering multistage or double-suction pumps with thick hubs, particular attention must also be paid to the specific speed n_q , since excessive D_1/D_2 ratios can lead to an extremely short outer streamline and relatively high vane loads. Critical n_q values already start at $n_q = 35$ ($\text{NS} = 1800$), when $v > 0.65$.

From the above it can be concluded that the improvement of the NPSH_3 value that can be achieved by replacing an overhung suc-

tion impeller pump by a double-suction pump might be very limited. However, the lower inlet velocity and a higher stiffness of the rotor with its two bearings offer certain advantages as far as reliability is concerned.

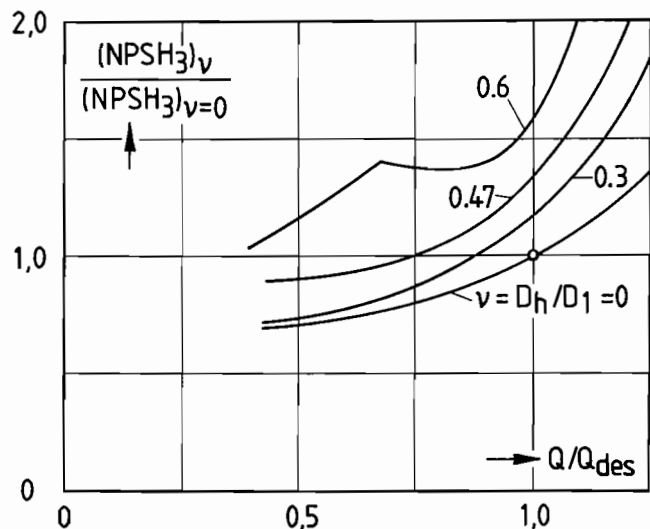


Figure 13. Influence of the Hub/Tip Ratio D_h/D_1 at the Impeller Inlet on $NPSH_3$ Test Results with an Overhung Impeller.

Table 2.

	Case 1	Case 2	Case 3	
$d = \text{double}$	$v_d = 0.45$	$v_d = 0.45$	$v_d = 0.6$	
$s = \text{single}$	$v_s = 0$	$v_s = 0.3$	$v_s = 0.6$	
A_d/A_s	1.17	1.21	1.26	
D_{1d}/D_{1s}	0.856	0.830	0.794	
$\frac{NPSH_{3d}}{NPSH_{3s}}$	0.73	0.69	0.63	$\sigma_{u_d} = \sigma_{u_s}$
$\frac{NPSH_{3d}}{NPSH_{3s}}$	0.96	0.77	0.63	Correction with Figure 13

Inducers

General Remarks

If the NPSHA value is so low that even the use of a suction impeller or double-suction pump does not yield satisfactory performance data, the designer of a pump station has to look for methods of raising the fluid's energy level upstream of the impeller.

One method consists in installing a separate booster pump (see *Booster Pumps*); another method, often used for single-stage volute casing pumps, is fitting an axial impeller stage, a so-called inducer, just before the main impeller. Inducers typically are axial or mixed-flow impeller stages without diffusers, which are arranged on the pump impeller shaft and therefore have the same speed and direction of rotation. The fact that the inducer is close to the impeller and in particular the swirling flow downstream of the inducer (= inflow to pump impeller) influence the impeller's operating characteristics, which means that the flow conditions are rather more complex than those for booster pump configurations.

The inducer is not expected to increase the pump's discharge head. The primary objective is the suppression of cavitation phenomena in the impeller; the inducer itself works in a distinct cavitation regime with a head drop of considerable proportion referred to the inducer's discharge head. The NPSH required by the inducer for proper pump operation is markedly lower than the pump impeller's $NPSH_3$ value. This situation is illustrated in Figure 14.

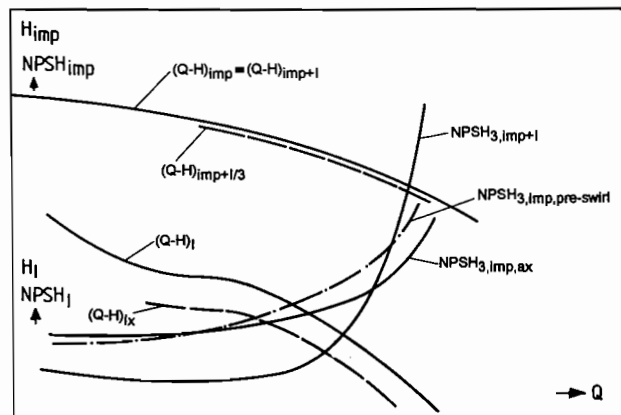


Figure 14. Head and NPSH Curves of a Pump with Inducer vs Flowrate for Different Operating Conditions. $(Q-H)_{imp}$ = main impeller only; $(Q-H)_I$ = inducer only; $(Q-H)_{imp+I/3}$ = impeller and inducer with three percent head drop; $(Q-H)_{I \times}$ = inducer with head drop of more than three percent (= \times percent); $NPSH_{3,imp,ax}$ = NPSH of the impeller with axial inlet flow; $NPSH_{3,imp,pre-swirl}$ = NPSH of the impeller with preswirl caused by an inducer.

A schematic pressure (energy) curve is shown in Figure 15 along a hypothetical streamline through the pump, with and without inducer, thus highlighting the benefit gained by using an inducer ($\Delta NPSH$).

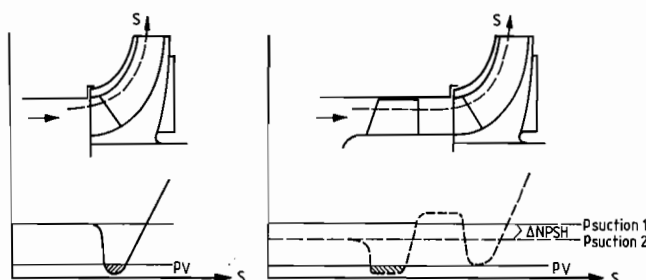


Figure 15. Pressure Distribution Along the Flow Path Through a Standard Pump with (Right) and Without Inducer (Left).

When designing an inducer or a pump fitted with an inducer, different approaches are required for the two cases outlined below:

- An inducer is to be fitted upstream of an existing pump impeller designed for operation without inducer (majority of cases, such as field retrofit).
- The inducer and the impeller are to be designed jointly for new applications.

An inducer, like any turbomachine, imparts mechanical energy to the fluid by way of its rotation and the resulting change in flow direction. This means that the axial inlet flow is deviated and leaves the inducer with swirl, which, in case, 1 will cause shock losses at the pump impeller inlet and may impair the inducer effect.

In case 2, such losses do not occur, and a well-matched inducer/impeller configuration will yield noticeably better results.

The use of an inducer (without diffuser) does not alter the total discharge head, as the simple consideration below demonstrates. According to Euler's equation the following applies:

$$H_{th} = \frac{u_2 \cdot c_{u2} - u_1 \cdot c_{u1}}{g} \quad (10)$$

At the inducer inlet $c_{u1} = 0$ (axial inlet flow), while the outlet swirl produced by the inducer enters the pump impeller inlet:

$$(u_2 c_{u2})_{inducer} = (u_1 c_{u1})_{impeller} \quad (11)$$

$$H_{th, inducer} = \frac{(u_2 \cdot c_{u2})_{inducer}}{g} \quad (12)$$

$$H_{th, impeller} = \frac{(u_2 \cdot c_{u2})_{impeller} - (u_2 \cdot c_{u2})_{inducer}}{g} \quad (13)$$

Thus, the increase in head generated by the inducer equals the head reduction of the pump impeller, and the total discharge head does not change when an inducer is used.

For the design of new inducers, often Equation (5) is applied for evaluating the suction characteristics. Depending on the type of pump and inducer, and apart from extreme cases for short periods of operation, values ranging between $\lambda w = 0.03 - 0.05$ can be achieved. In the following table, the S_q values are listed which can be achieved with the individual designs to improve the suction behavior:

The inducer may be designed like an axial pump impeller. Two designs have proved to be particularly effective:

- axial impeller with continuously changing vane angle along a streamline and
- axial impeller with constant vane angle.

Table 3.

S_q (NSS)	=	220 - 230	(11,000 - 12,000)	standard impeller
S_q (NSS)	=	300 - 315	(15,500 - 16,300)	suction impeller
S_q (NSS)	=	350	(18,000)	double-suction impeller
S_q (NSS)	=	450	(23,000)	inducer
S_{qmax} (NSS)	=	700	(36,000)	inducer

The second option is often preferred because of its low manufacturing cost. Since this type of inducer can only generate head by an incidence, the vane angle at the outer streamline is designed three to six degrees larger than the inlet flow angle. Combined with the effect of the inducer's low number of vanes ($z = 2 \div 4$), this design ensures that the inducer's discharge head will only be affected by vapor bubble formation on the vane in an advanced stadium (i.e., at an extremely low NPSH value).

In Figure 16, the relationship between the NPSH curves of a volute casing pump with and without inducer and various inducer vane angles is shown.

If the inducer is designed with a variable vane angle, which enables incidence-free inlet flow at the design point, the inducer's NPSH value will be improved and its efficiency will be substantially increased, in particular in the overload range (Figure 17).

Inducer Types

The simplest inducer design is in fact an axial pump impeller, which is arranged on the extended shaft upstream of the main pump impeller (Figure 18). Its diameter is identical to the impeller inlet diameter.

This design is predominantly chosen when the impeller is a suction impeller, which by definition already has a large inlet diameter. If a standard impeller pump is to be retrofitted with an inducer, the inducer diameter should be larger than D_1 (Figure 18 (b)). Double inducers as shown in Figure 18 (d) have a narrow operating range, and also extremely high suction specific speeds ($S_q \approx 1100$; $NSS \approx 57,000$).

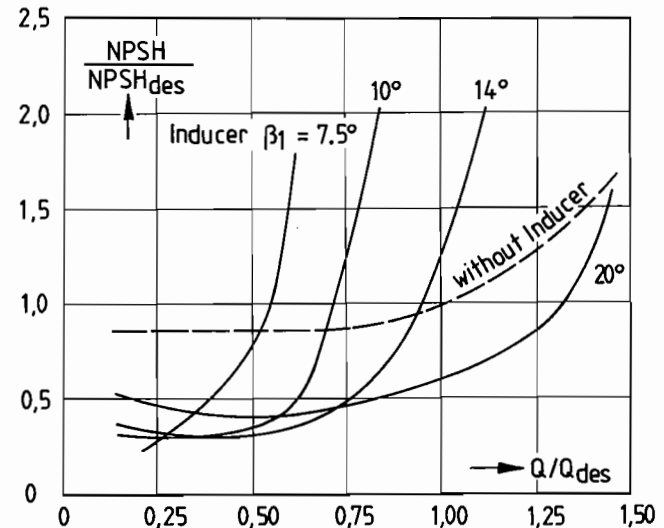


Figure 16. NPSH Curves of a Pump with and without Inducer and Various Inducer Blade Angles vs Relative Flowrate.

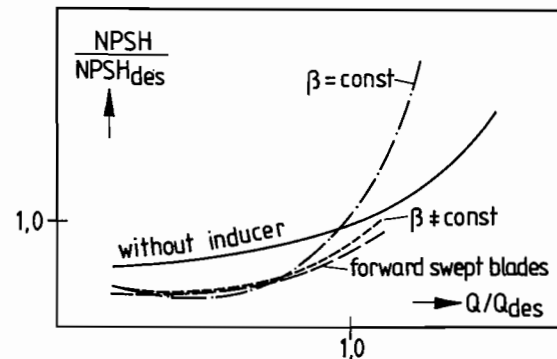


Figure 17. NPSH Curves of a Pump Equipped with Inducers of Different Design Compared with a Pump without Inducer.

With a view to enhancing inducer efficiency even more, a number of measures have been tested and adapted to meet the specific requirements of actual pumping application. The following list outlines starting points for further improvement:

- profiling the inducer vanes to reduce the pressure drop at the inducer inlet,
- a conical hub to increase the inducer's discharge head (Figure 18(c)),
- an inducer with, for example, three long and three short vanes to achieve the same goal,
- an upstream and/or downstream diffuser, with the latter improving the impeller's inlet flow.

In some cases, an inducer with a separate, lower-speed drive can further improve conditions. But this solution is very expensive, of course.

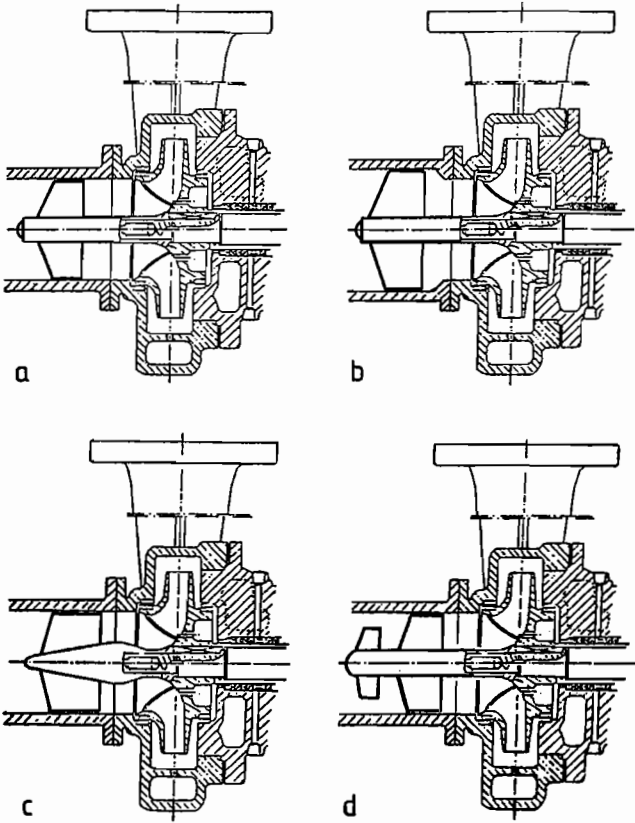


Figure 18. Different Types of Inducers a) common type; b) with enlarged o. d. c) with a conical hub; d) double inducer.

For a comprehensive consideration of the behavior of an inducer it should be mentioned that low flow operation may give rise to certain problems. In this operation range ($Q < 0.2 \cdot Q_{opt}$), a phenomenon called surging may develop, i.e., pressure (and flowrate) fluctuations caused by a periodic blockage of the inducer inlet by a cavitation cloud.

The consequences of these phenomena limiting the operating range can be avoided or at least abated by the measures described in *Improvements in the Low-Flow Range*. In all, it is difficult to state an exact limit, because this depends very much on the particular hydraulic design and, because not all potential influencing parameters are known.

BOOSTER PUMPS

If, for example in the case of large boiler feed pumps with given Q and H , economic aspects call for high-speed units ($n = 5000$ to 6000 rpm) and if even the use of suction stage impellers, double-suction impellers or inducers cannot ensure reliable, damage-free operation at a given NPSHA, the only feasible option is to install a booster pump with lower speed. Its discharge head must be matched to the main pump's NPSH requirement, which in turn depends on the permissible cavitation zone length (see *Cavitation Erosion*). In extreme cases, the following is required:

$$(NPSH)_B + H_B \geq (NPSH_i)_M$$

where $(NPSH_i)_M$ must be as small as possible to keep total pump unit costs down. The development of special vane profiles [8] and modern manufacturing methods [9] have made a vital contribution to substantial progress in this field over the last few years.

The development stages are illustrated in Figure 19 of a 50 percent load boiler feed pump, installed in a 1300 MW nuclear power station. The upper limit of the ratio D_{2B}/D_{2M} between the diameters of booster and main pump is assumed to be 1.75 for economic reasons. The second limit $(D_1/D_2)_M \leq 0.65$ refers to the main pump whose specific speed n_q should not be higher than 35 ($N_S = 1800$). At higher specific speeds, the risk of characteristic curve instabilities in the $Q/Q_{opt} = 0.6$ to 0.7 range increases, and the higher loads on the vanes (see above) impair $NPSH_i$. In this case, the economically and physically reasonable limit seems to range at about 6000 min^{-1} [10].

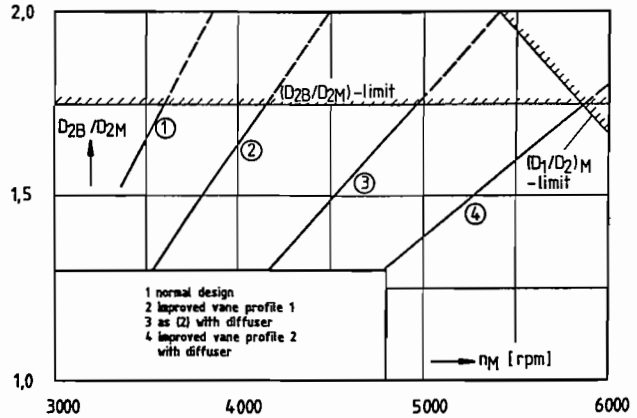


Figure 19. Improved Boiler Feed Pump for a Given Limit of the Diameter Ratio between Booster Pump and Main Pump D_{2B}/D_{2M} .

IMPROVEMENTS IN THE LOW-FLOW RANGE

As far as operation of a pump in the low flow range $Q < Q_{des}$ is concerned, a fundamental distinction must be made between two cases: $Q_{des} > Q > Q_{IR}$, i.e., there is no evidence of inlet recirculation at the impeller vanes, or $Q < Q_{IR}$ with increasingly intensive recirculation towards $Q = 0$. It must also be examined whether the actual cavitation intensity would in fact cause erosion damage or not. If not, further investigation is not required, since according to Stoffel and Jaeger [11] the impeller design has but a minor influence on the mechanical operating behavior.

If cavitation erosion is a problem, vane profiles, as illustrated in Figure 4, improve conditions in the $Q_{des} > Q > Q_{IR}$ range to a limited extent only.

A marked improvement compared with standard profiles is described by Hergt [12]. A special vane design at the inlet helps keep the value for incipient cavitation in the low flow range at the design point level (Figure 20).

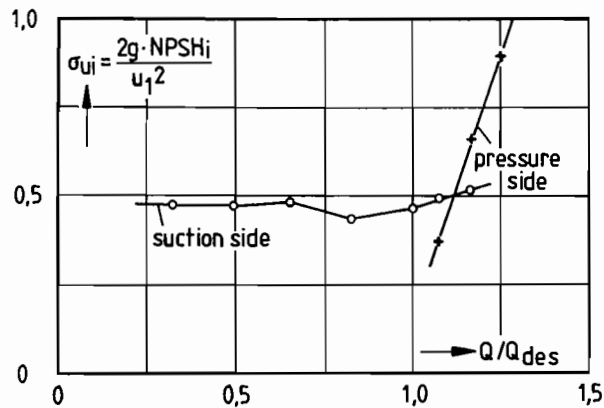


Figure 20. Cavitation Coefficient σ vs Flowrate for Improved Vane Profile.

Although these measures only alter $NPSH_1$, with $NPSH_3$ remaining more or less constant, they do affect cavity growth in such a way that the cavitation zone length reduced on account of cavitation erosion effects is reached at lower NPSH values compared with standard profiles (Figure 21). This means that the cavitation erosion at any $NPSH_A$ between $NPSH_1$ and $NPSH_3$ will be less pronounced.

Before discussing potential measures for improving operation at $Q > Q_{IR}$, it would have to be examined whether a specific machine enters this regime at all. In other words, the recirculation inception point Q_{IR} for a given geometry would have to be localized. Various attempts have been made to solve this issue [e.g., 13, 14, and 15], which to the knowledge of the authors have not yet yielded satisfactory results however. Starting from very generalizing hypotheses that only consider a few of the possible influencing parameters, relationships have been derived by Fraser [7] to compute the onset of recirculation using only a few geometric pump parameters. These were further simplified [13], where the critical value Q_{IR}/Q_{des} is correlated directly with the suction specific speed $(NSS)_3$. The statement is that the higher S_{q3} is, the larger the relative flowrate at recirculation onset is, i.e., the smaller the safe operating region (Figure 22). The tendency illustrated in this figure can be confirmed with certainty, but apparently the correlations as such are not so easy to define.

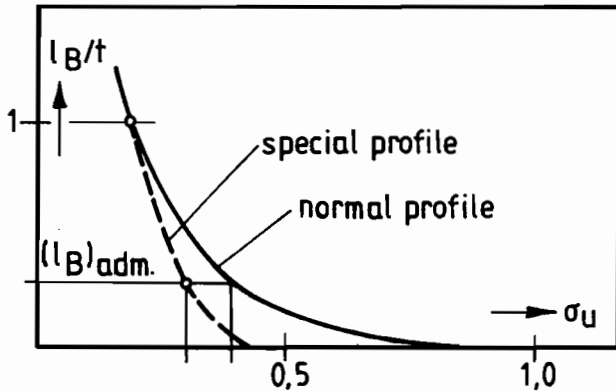


Figure 21. Cavity Length vs NPSH for Different Vane Profiles.

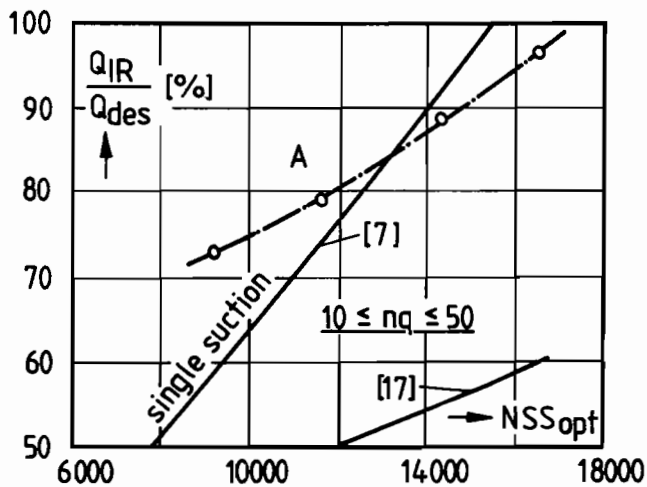


Figure 22. Onset of Inlet Recirculation Q_{IR}/Q_{des} vs Specific Suction Speed.

In Figure 22, which was taken from Stoffel and Hergt [16], several measurements done in-house at KSB have been plotted. Curve A was obtained in a set of experiments in which four impellers dif-

fering only in inlet diameter and corresponding vane angle were tested. The trend is very similar to the original curve, but the level is different. This results from the conclusion, which was for example also drawn by Schiavello [14] and Sen [15], that β_1 is only one of many parameters which determine Q_{IR} . Another parameter apparent in Schiavello [14] and Sen's [15] work is the location of the leading edge relative to the axial direction, which according to our own measurements may lead to differences in Q_{IR} of up to 40 percent, keeping other parameters constant. In this light, it is understandable that a curve given by Palgrave [17] ranges at a completely different level.

Nonetheless, it can be assumed that at a given flowrate, Q , and speed, n , larger inlet diameters (higher δ and smaller β_1) will result in higher Q_{IR} values and according to Equation $(P_{IR} \sim \delta^5)$ also in intensified recirculatory flows.

Although cavitation within the recirculation zone starts to develop at a markedly lower $NPSH_A$ value than vane cavitation, as illustrated in Figure 5, little is known about its intensity. Therefore, it is recommended to take appropriate measures to improve conditions in general.

Diffuser Upstream of the Impeller

Hergt, Jaberg, and Amann [18] demonstrated that a diffuser fitted upstream of the impeller has a major influence on the recirculation zone length. The correlation illustrated in Figure 23 is between the diffuser and recirculation zone lengths, L_D , and L_{IR} , respectively. At a flowrate corresponding to $c_{m0}/u_1 = 0.1$, the following applies:

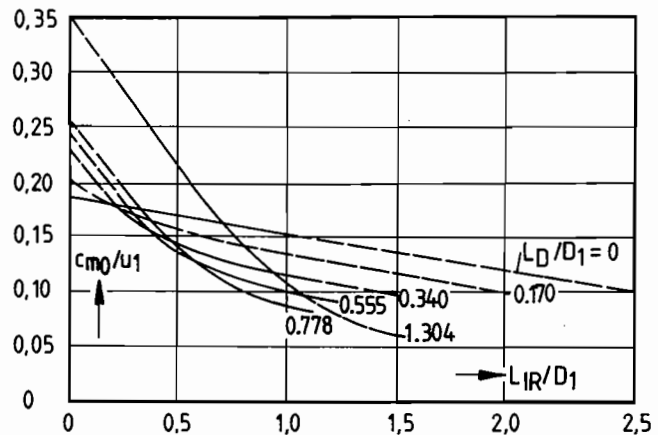


Figure 23. Influence of the Length L_D of an Inlet Diffuser on the Extension of the Recirculation Zone L_{IR} .

The axial extension of the inlet recirculation zone is $L_{IR} = 2.5 \cdot D_1$ without and $0.8 \cdot D_1$ with a diffuser having a length of $L_D = 0.778 \cdot D_1$.

It has been additionally demonstrated by Hergt and Hellmann [19] that the diffuser considerably influences the velocity distribution within and outside the recirculation zone. The axial and tangential velocity components within the backflow are much smaller than without the diffuser. In contrast, the flow approaching the impeller has a higher tangential component resulting in a smaller angle of incidence near the hub.

Hence, the ratio of the power transferred in the recirculatory flow at $Q = 0$ with and without diffuser is

$$\frac{(P_{IR})_{diff}}{(P_{IR})_{norm}} \approx 0.3$$

and that of the circulating volume flows

$$\frac{(Q_{IR})_{diff}}{(Q_{IR})_{norm}} \approx 0.5$$

This means that a diffuser reduces the recirculation intensity substantially. The conclusion, corroborated by practical experience, is that the cavitation risk is considerably lower. The diffuser effect is also reflected in the values for incipient cavitation, in particular at $Q < Q_{IR}$, as illustrated in Figure 24.

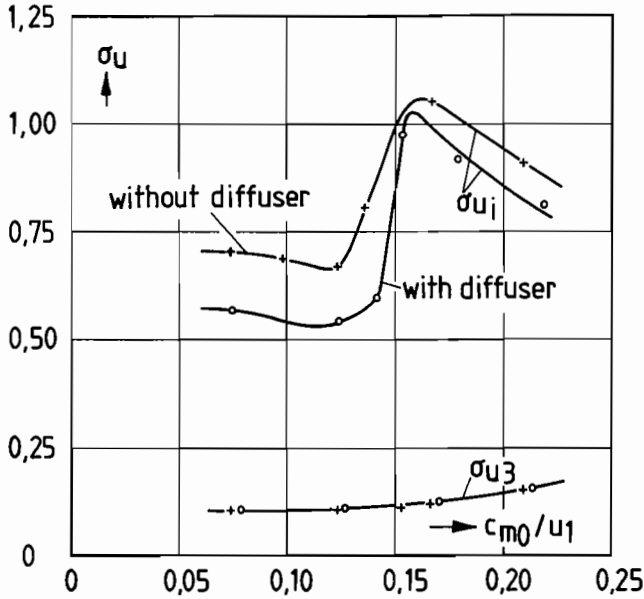


Figure 24. Comparison of σ_{ui} and σ_{u3} without and with a Diffuser ($2\alpha = 14$ degrees).

Swirl Control

Another effect caused by recirculation, which may result in a reduced operating range, is shown in Figure 25, where the difference between the local static pressure immediately upstream of the impeller and the pressure far upstream at $Q = 0$ is plotted. Owing to the circumferential component in the recirculation zone the pressure decreases radially inwards and reaches considerably negative values near the hub. If NPSHA is low, this may cause the medium to evaporate near the hub (pipe center), which in turn may bring on the well-known phenomenon of low-frequency auto-oscillation with considerable head fluctuations. Although the low pressure recovers with increasing flowrate, it only reaches zero level at $Q \approx Q_{IR}$.

Various methods of preventing auto-oscillation are available, which, in the final analysis, are all based on eliminating the circumferential component of the recirculating flow. A solution was suggested in Kasztejna, et al. [20]. The recirculating flow from the impeller is led into a ring element equipped with vanes ending in axial direction. The flow is deswirled and reintroduced into the impeller. Since the flow does no longer have a circumferential component, the low pressure area in the center disappears and auto-oscillation is prevented.

A special solution examined by the authors is illustrated in Figure 26. It differs from Kasztejna, et al. [20], in the method of reintroducing the recirculating flow and the use of a diffuser. Although a direct comparison has not been made yet, it is expected to be slightly more effective.

The same conceptual approach can be applied without great effort and outlay to can-type pumps, which are mostly installed vertically (Figure 27). Just upstream of the impeller, the inlet pipe

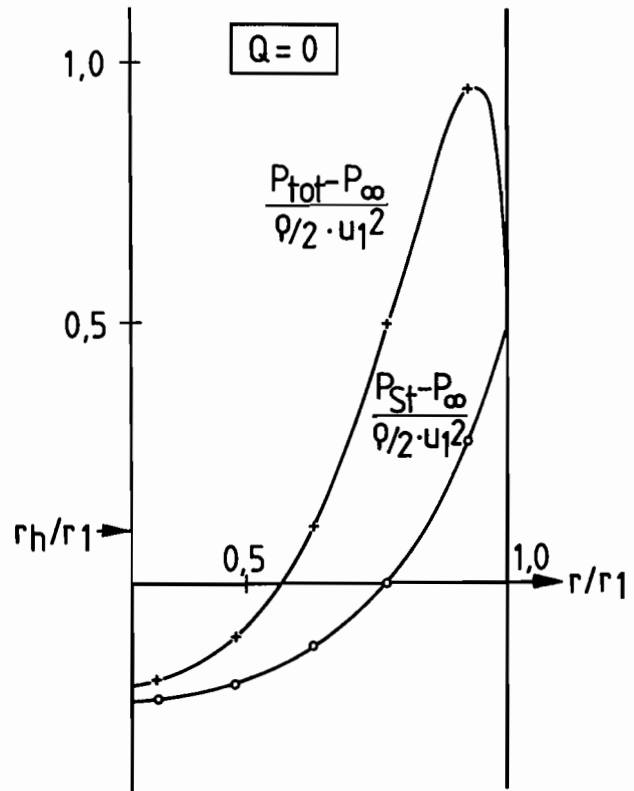


Figure 25. Total and Static Pressure Distribution Upstream of the Impeller at Shutoff Point.

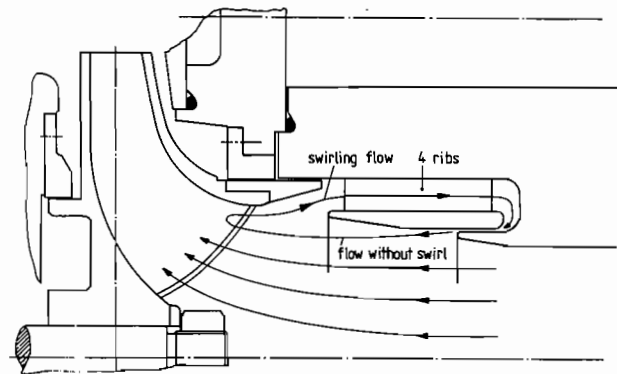


Figure 26. Pump Provided with Annular Slot and Vanes Upstream of the Impeller.

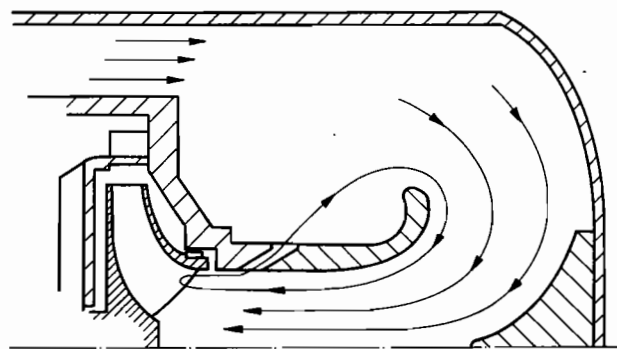


Figure 27. Inlet Pipe with Slot in Front of a Pump.

is equipped with an diagonal slot allowing the recirculating flow to escape into the clearance between can and suction pipe. With an adequately dimensioned slot, this method eliminates auto-oscillation almost completely.

These measures can obviously only be effective, if the recirculating flow enters the slot or the ring element. Some impellers, for example, those with inlet edges approximately parallel to the axis show comparatively short axial extensions of the recirculation zone, which may not be influenced by the measures mentioned above. However, all the negative consequences of inlet recirculation, e.g., those explained in Figure 25, will be much less pronounced.

Recirculation Suppression

Sometimes, a pump is found to operate in the low flow range most of the time after it has been commissioned. In these cases, a simple method of adapting the impeller to the actual operating conditions is available. It consists in retrofitting a ring that reduces the inlet diameter (Figure 28 (a)). This ring extends into the vaned part of the impeller and 'cuts off' a partial flow impeller, so to speak. Q_{IR} is shifted to lower flowrates and the recirculatory flow is less intensive. In some cases, an orifice was fitted upstream of the impeller (Figure 28 (b)). An orifice is very easy to install and has a similar effect, but it is less effective. Although it does not prevent recirculation, it keeps the axial extension of the recirculation zone short and reduces the power consumption.

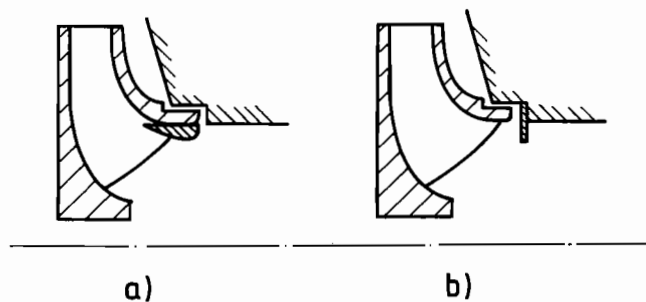


Figure 28. Orifice within the Impeller Eye (a) or in Front of it (b).

SUMMARY

- On the basis of a brief explanation of the basic flow phenomena within an impeller, the general cavitation performance of a pump is described.
- limits of the suction capability as a function of the particular impeller design and the overall pump design (single-suction, double-suction, etc.) and as the related operational restrictions are outlined.
- Maximum suction specific speeds, which are given in this contribution, enable planners and users to pinpoint the suitable solution for a specific application or to assess whether there is a chance of meeting the requirements at all.
- It is also demonstrated that the trouble, which could be expected at very reduced flowrates, can be avoided or at least moderated by taking certain measures at the pump inlet.

NOMENCLATURE

A	(m)	area
c	(m/s)	absolute velocity
c_m	(m/s)	meridional velocity
D	(m)	diameter
E_R	(mm/h)	erosion rate
H	(m)	head

HCI		hydrodynamic cavitation intensity
I_B	(m)	cavitation zone or bubble length
L_D	(m)	diffuser length
n	(rpm)	rotational speed
NPSH	(m)	net positive suction head
NPSHA	(m)	NPSH available
n _q	(rpm)	specific speed
N_s	(rpm)	specific speed
NSS	(rpm)	suction specific speed
P	(kW)	input power
PS		pressure side
Q	(m ³ /s)	flowrate
S_q	(rpm)	suction specific speed
SS		suction side
t	(m)	pitch
u	(m/s)	circumferential velocity
w	(m/s)	relative velocity
z	(-)	vane number
α	(°)	diffuser angle
β	(°)	impeller vane angle
δ	(m)	specific inlet number
λ_c	(-)	coefficient
λ_w	(-)	coefficient
σ_u	(-)	cavitation coefficient

INDICES

bd	head breakdown
B	booster pump
BEP	best efficiency point
cf	cavitation-free
crit	critical
des	design
h	hub
i	incipient
IR	inlet recirculation
M	main pump
opt	optimum efficiency
req	required
th	theoretical
u	tangential
o	upstream of the impeller
1	inlet
2	outlet
3	3.0 percent head drop

REFERENCES

1. Kosyna, G., et al., "NPSH_R of Mixed-flow Pumps at Part-load Operating Conditions," Proc. of the Int. Symposium on Cavitation, Deauville/France, pp. 15-21 (1995).
2. Fang, K. S., Discontinuity of H-Q-Curve as Affected by Available NPSH, Cavitation and Polyphase Forum, Montreal, Edited by R. L. Waid (1974).
3. Massey, I. C., "The Suction Instability Problem in Rotodynamic Pumps," Proc. of the Int. Conf. on Pump and Turbine Design and Development, East Kilbride (1976).
4. Feedpump Operation and Design Guidelines, Summary Report on EPRI Research Project 1884-10.
5. Schiavello, B., Sen M., "On the Prediction of the Reverse Flow Onset at the Centrifugal Pump Inlet," Proc. of the 22nd Annual Fluids Engineering Conference, New Orleans, pp. 261-272 (1980).
6. Pfeleiderer, C., Die Kreiselpumpen für Flüssigkeiten und Gase, Springer-Verlag, Berlin, Göttingen, Heidelberg (1961).

7. Fraser, W. H., "Recirculation in Centrifugal Pumps," World Pumps, pp. 227-235 (1982).
8. Krieger, P., Spezielle Profilierung an Laufrädern von Kreiselpumpen zur Senkung von $NPSH_i$, VGB Kraftwerkstechnik 72, pp. 395-398 (1992).
9. Riegger, H. and Nicklas, A., "Modern Manufacturing of Advanced Impeller and Diffuser Vane Profiles," *Proceedings of the Twelfth International Pump Users Symposium*, Turbomachinery Laboratory, Texas A&M University, College Station, Texas, pp. 37-46 (1995).
10. Hergt, P., et al. "Status of Boiler Feed Pump Development," Proc. from 15th IAHR-Symposium, Belgrade/Yugoslavia (1990).
11. Stoffel, B. and Jaeger, R., "Experimental Investigations in Respect to the Relevance of Suction Specific Speed for the Performance and Reliability of Centrifugal Pumps," *Proceedings of the Thirteenth International Pump Users Symposium*, Turbomachinery Laboratory, Texas A&M University, College Station, Texas (1996).
12. Hergt, P., "Design Approach for Feed Pump Suction Impellers," Power Plant Pump Symposium, Tampa, Florida (1991).
13. Fraser, W. H., "Flow Recirculation in Centrifugal Pumps," *Proceedings of the Tenth Turbomachinery Symposium*, Turbomachinery Laboratory, Texas A&M University, College Station, Texas, pp. 95-100 (1981).
14. Schiavello, B., "A Diffusion Factor Correlation for the Prediction of the Reverse Flow Onset at the Centrifugal Pump Inlet," Seventh Conference on Fluid Machinery, Budapest, pp. 751-760 (1983).
15. Sen, H. M., "Prediction of the Reverse Flow and Prerotation in Centrifugal Pumps," Seventh Conference on Fluid Machinery, Budapest, pp. 805-814 (1983).
16. Stoffel, B., Hergt, P., Zur Problematik der spezifischen Saugzahl als Beurteilungsmaß für die Betriebssicherheit einer Kreiselpumpe, Pumpentagung Karlsruhe, pp. 77-81 (1988).
17. Palgrave, R., "Avoid Low Flow Pump Problems," The Proceedings of the twelfth International Pump Technical Conference, London, pp. 124-139 (1991).
18. Hergt, P., Jaberg, H. and Amann, P., "Influence of a Diffuser in Front of a Radial Impeller on Its Performance," Proceedings of the eighth Conference on Fluid Machinery, Budapest (1987).
19. Hergt, P. and Hellmann, D., "Velocity and Energy Distribution in Front of the Impeller of a Centrifugal Pump Operating under Part-load Conditions," Proceedings of the Sixth Conference on Fluid Machinery, Budapest (1979).
20. Kasztejna, P. J., Heald, C. C., and Cooper, P., "Experimental Study of the Influence of Backflow Control on Pump Hydraulic-Mechanical Interaction," *Proceedings of the Second International Pump Users Symposium*, Turbomachinery Laboratory, Texas A&M University, College Station, Texas (1985).